Colletotrichum higginsianum extracellular LysM proteins play dual roles in appressorial function and suppression of chitin-triggered plant immunity.

Hiroyuki Takahara, Stéphane Hacquard, Anja Kombrink, H Bleddyn Hughes, Vivek Halder, Guillaume Robin, Kei Hiruma, Ulla Neumann, Tomonori Shinya, Erich Kombrink, et al.

Colletotrichum higginsianum extracellular LysM proteins play dual roles in appressorial function and suppression of chitin-triggered plant immunity

Hiroyuki Takahara[1]*, Stéphane Hacquard[1]*, Anja Kombrink[2], H. Bleddyn Hughes[1], Vivek Halder[3], Guillaume P. Robin[4], Kei Hiruma[1], Ulla Neumann[5], Tomonori Shinya[6], Erich Kombrink[3], Naoto Shibuya[6], Bart P. H. J. Thomma[2] and Richard J. O'Connell[1,4]

[1]Department of Plant–Microbe Interactions, Max-Planck-Institute for Plant Breeding Research, 50829 Cologne, Germany; [2]Laboratory of Phytopathology, Wageningen University, Droevendaalsesteeg 1, 6708 PB, Wageningen, the Netherlands; [3]Chemical Biology Laboratory, Max-Planck-Institute for Plant Breeding Research, 50829 Cologne, Germany; [4]UMR BIOGER, INRA, AgroParisTech, Université Paris-Saclay, 78850 Thiverval-Grignon, France; [5]Central Microscopy, Max-Planck-Institute for Plant Breeding Research, 50829 Cologne, Germany; [6]Department of Life Sciences, School of Agriculture, Meiji University, Kawasaki 214-8571, Japan

Author for correspondence:
Richard J. O'Connell
Tel: +33 0 1 30 81 45 82
Email: richard.oconnell@versailles.inra.fr

Summary

• The genome of the hemibiotrophic anthracnose fungus, *Colletotrichum higginsianum*, encodes a large repertoire of candidate-secreted effectors containing LysM domains, but the role of such proteins in the pathogenicity of any *Colletotrichum* species is unknown.

• Here, we characterized the function of two effectors, ChELP1 and ChELP2, which are transcriptionally activated during the initial intracellular biotrophic phase of infection.

• Using immunocytochemistry, we found that ChELP2 is concentrated on the surface of bulbous biotrophic hyphae at the interface with living host cells but is absent from filamentous necrotrophic hyphae. We show that recombinant ChELP1 and ChELP2 bind chitin and chitin oligomers *in vitro* with high affinity and specificity and that both proteins suppress the chitin-triggered activation of two immune-related plant mitogen-activated protein kinases in the host *Arabidopsis*. Using RNAi-mediated gene silencing, we found that *ChELP1* and *ChELP2* are essential for fungal virulence and appressorium-mediated penetration of both *Arabidopsis* epidermal cells and cellophane membranes *in vitro*.

• The findings suggest a dual role for these LysM proteins as effectors for suppressing chitin-triggered immunity and as proteins required for appressorium function.

Introduction

Colletotrichum higginsianum is an ascomycete fungus causing anthracnose disease of many cultivated Brassicaceae as well as the model plant *Arabidopsis thaliana* (O'Connell *et al.*, 2004). *C. higginsianum* uses a multistage, hemibiotrophic infection strategy to invade host plants: the fungus first penetrates the host cuticle and cell wall by means of melanized appressoria, and then, during the subsequent biotrophic stage, bulbous primary hyphae resembling haustoria develop inside living host epidermal cells enveloped by an intact host plasma membrane (O'Connell *et al.*, 2004). Later, the fungus switches to destructive necrotrophy, associated with the differentiation of thin, filamentous secondary hyphae that secrete a cocktail of lytic enzymes, leading to host tissue destruction (O'Connell *et al.*, 2012).

The *C. higginsianum* genome was recently sequenced, providing the opportunity to study the genetic determinants controlling these pathogenic transitions (O'Connell *et al.*, 2012). In particular, the early stages of infection (appressorial penetration and biotrophy) are marked by the activation of a large array of genes encoding putative secreted effector proteins (Kleemann *et al.*, 2012; O'Connell *et al.*, 2012), which potentially interfere with or suppress plant immune responses to enhance pathogen growth (Stergiopoulos & de Wit, 2009). Analysis of the *C. higginsianum* genome sequence revealed an unusually large number of genes (22) encoding proteins containing CBM50 modules, surpassing most other fungi examined so far (O'Connell *et al.*, 2012). This protein domain, also known as the LysM or lysin motif, comprises 40–60 amino acid residues and mediates binding to chitin and peptidoglycans (de Jonge & Thomma, 2009). Chitin, a β-1,4-linked homopolymer of *N*-acetylglucosamine, is an essential structural component in the cell walls of all fungi, comprising 10–20% of the wall by dry weight (Bowman & Free, 2006).

Chitin is a microbe-associated molecular pattern (MAMP) that can be detected by plant pattern recognition receptors (PRRs) to activate a variety of MAMP-triggered immune

*These authors contributed equally to this work.

responses (Dodds & Rathjen, 2010). All the plant PRRs known to be involved in chitin recognition are LysM-containing proteins localized in the plasma membrane. In *Arabidopsis thaliana*, the LysM receptor-like kinase LYK1/CERK1 (chitin elicitor receptor kinase 1) is essential for chitin recognition and signalling (Miya *et al.*, 2007). More recently, two other LysM receptor-like kinases, LYK4 and LYK5, were shown to be required for chitin signalling and may form a chitin-induced receptor complex together with LYK1/CERK1 (Cao *et al.*, 2014). In addition, LYM2, an *Arabidopsis* homologue of the rice chitin receptor CEBiP (Chitin Elicitor Binding Protein 1; Kaku *et al.*, 2006), binds chitin oligosaccharides with high affinity and contributes to defence against some fungal pathogens via a LYK1/CERK1-independent pathway (Shinya *et al.*, 2012; Faulkner *et al.*, 2013; Narusaka *et al.*, 2013).

To evade recognition by host chitin receptors, several phytopathogenic ascomycetes secrete effector proteins which either compete with the host receptors for binding chitin fragments or reduce the accessibility of cell wall chitin to attack by plant chitinase enzymes which release chitin fragments (Sánchez-Vallet *et al.*, 2015). The biotrophic pathogen *Cladosporium fulvum*, causal agent of tomato leaf mould, proliferates as an intercellular mycelium and secretes the effector Avr4, which contains an invertebrate type chitin-binding domain rather than LysM domains. Through binding to chitin, Avr4 was shown to protect fungal cell walls against plant chitinases (van den Burg *et al.*, 2006; van Esse *et al.*, 2007). In addition, an extracellular LysM domain-containing protein called Ecp6 was identified from *C. fulvum* apoplastic fluids (Bolton *et al.*, 2008). This protein is highly expressed *in planta*, has the ability to bind chitin and suppresses chitin-triggered defense responses by sequestering chitin fragments, thereby preventing their recognition by plant chitin receptors (de Jonge *et al.*, 2010; Sánchez-Vallet *et al.*, 2013). Similarly, the secreted LysM domain protein Slp1 from the rice blast fungus *Magnaporthe oryzae* was shown to compete for binding chitin fragments with the rice CEBiP receptor (Mentlak *et al.*, 2012). Two additional LysM effectors (Mg1LysM and Mg3LysM) were characterized in the Septoria leaf blotch pathogen, *Mycosphaerella graminicola* (Marshall *et al.*, 2011) which, like *C. fulvum*, proliferates entirely intercellularly. Similar to Slp1 and Ecp6, Mg3LysM interferes with chitin recognition by CERK1 and CEBiP homologues in wheat (Lee *et al.*, 2014), but both *M. graminicola* LysM effectors also protect fungal hyphae against plant chitinases (Marshall *et al.*, 2011), similar to *C. fulvum* Avr4. All the above-mentioned LysM effectors were shown to contribute to fungal virulence, indicating a conserved function among plant pathogenic ascomycetes of the families Mycosphaerellaceae (Dothideomycetes) and Magnaporthaceae (Sordariomycetes).

The first report of a fungal secreted LysM protein was CIH1 from the bean anthracnose fungus *Colletotrichum lindemuthianum* (Perfect *et al.*, 1998). Using immunocytochemistry, CIH1 was located on the intracellular biotrophic hyphae of this pathogen (Pain *et al.*, 1994). However, it remains unclear whether secreted LysM proteins play a role in the virulence of any *Colletotrichum* species. Here, we characterized two homologs

of CIH1 from *C. higginsianum*, namely *C. higginsianum* extracellular LysM proteins 1 and 2 (ChELP1 and ChELP2, respectively), which are similarly secreted during the biotrophic phase of infection. We show that both proteins bind chitin oligomers and polymer with high affinity *in vitro* and that they are essential for full pathogenicity. Evidence is presented that the proteins play a dual role, not only in the suppression of chitin-triggered immune responses but also in appressorium function.

Materials and Methods

Fungal and plant material

The genome-sequenced *C. higginsianum* isolate IMI349063A (O'Connell *et al.*, 2012) was used for all experiments and as parental strain for fungal transformations. Fungal cultures and *Arabidopsis thaliana* Col-0 plants were grown as described previously (Huser *et al.*, 2009). The following *Arabidopsis* mutants were also used (all in the Col-0 background): *cerk1-2* (Miya *et al.*, 2007), *lym2-1* and the *lym1-1 lym2-1 lym3-1* triple mutant (Shinya *et al.*, 2012). For pathogenicity assays, plants were spray-inoculated with conidial suspension (Huser *et al.*, 2009). For immunofluorescence microscopy and RNA-sequencing experiments, conidial suspensions were applied to the abaxial surface of detached *Arabidopsis* leaves (Takahara *et al.*, 2009).

Structure and phylogeny of ChELPs

Colletotrichum higginsianum extracellular LysM proteins were predicted as extracellular proteins using SignalP (v.4.0, Petersen *et al.*, 2011). Protein domain organization, including LysM domain prediction, was determined using the pfam database (http://pfam.xfam.org/, Punta *et al.*, 2012). The phylogeny of the ChELPs was constructed based on a multiple alignment of full-length amino acid sequences using ClustalW (now Clustal Omega, http://www.ebi.ac.uk/Tools/msa/clustalo/, Larkin *et al.*, 2007). The resulting alignment was then used to generate a neighbour-joining tree in Mega4.1 (http://www.megasoftware.net/, Tamura *et al.*, 2007). The alignment of LysM protein sequences from ascomycete fungi was generated using ClustalW and edited in Jalview (http://www.jalview.org/, Waterhouse *et al.*, 2009).

RNA and DNA isolation

For reverse transcription quantitative polymerase chain reaction (RT-qPCR) assays, total RNA was isolated using the RNeasy Plant Mini kit (Qiagen) from seven fungal developmental stages that were previously described (Kleemann *et al.*, 2012) and vegetative mycelium was grown in Mathur's liquid medium for 5 d at 25°C with shaking (130 rpm). A DNase I (Qiagen) treatment was included during the RNA isolation procedure to eliminate traces of genomic DNA. RNA quality was checked using the Agilent 2100 Bioanalyzer (Agilent Technologies, Böblingen, Germany). To quantify fungal biomass *in planta*, genomic DNA was isolated from infected *Arabidopsis* leaves at 84 h postinoculation (hpi) using the DNeasy Plant Mini Kit (Qiagen).

Quantitative PCR

For RT-qPCR assays, first-strand cDNA was synthesized from 1 μg DNase-treated total RNA using the iScript cDNA synthesis kit (Bio-Rad) in a total volume of 20 μl. Amplification parameters were identical to those previously described (Hacquard *et al.*, 2012). Specific primers amplifying transcripts of *ChELP1* (CH063_13023), *ChELP2* (CH063_04445), extracellular matrix protein *ChEMP1* (CH063_02408, Takahara *et al.*, 2009), the glucose-6-phosphate 1-dehydrogenase *ChG6PDH* (CH063_10848) and the elongation factor 1-alpha *ChElF* (CH063_14343) were designed with Primer 3 and Amplify 3X programs and a BLASTN search was performed against the *A. thaliana* genome sequence to verify the absence of cross-annealing. Primer efficiency, ranging between 92% and 115%, was determined for each target sequence (Supporting Information Table S1). Expression data were normalized to the reference genes alpha-tubulin (*ChαTUB*, CH063_01222) and actin (*ChACT*, CH063_05065), as previously described (Kleemann *et al.*, 2012). To measure fungal biomass, 10 ng genomic DNA was used to amplify the *ChACT* fragment and DNA amounts were normalized to the *A. thaliana* actin 2 fragment (*AtACT*, AT3G18780). Primer pairs used for amplification of *ChACT* and *AtACT* were described previously (Lu *et al.*, 2009; Kleemann *et al.*, 2012). Experiments were performed in triplicate.

RNA sequencing

Fungal developmental stages, library preparation and data processing were previously described (O'Connell *et al.*, 2012). Heatmaps of gene expression profiles were generated using the Genesis expression analysis package (Sturn *et al.*, 2002). To derive the expression patterns of *ChELP* genes, relative expression indices were calculated as the ratio between the normalized number of reads for each gene at a given fungal stage and the geometrical mean number of reads calculated across the four stages (Duplessis *et al.*, 2011).

Expression of recombinant ChELPs, analysis of glycosylation and cross-reactivity with antibody UB25

Expression of ChELP1 in *Pichia pastoris* or *Escherichia coli* and ChELP2 in *P. pastoris* is described in Methods S1. Recombinant ChELP proteins were analysed by sodium dodecyl sulphate polyacrylamide gel electrophoresis (SDS-PAGE) and the specificity of mouse monoclonal antibody (MAb) UB25 was tested by Western blot using recombinant ChELP1 and ChELP2 proteins (Methods S2). The *Pichia*-expressed proteins were also used to determine the presence of mannosylated glycans (Methods S3).

Light microscopy and immunofluorescence

Trypan blue-lactophenol staining and clearing of infected leaf tissues for light microscopy have been described previously (Takahara *et al.*, 2009). To quantify appressorial penetration, *Arabidopsis* leaves were cleared in ethanol : chloroform (3 : 1), mounted on slides in lactophenol and viewed by differential interference contrast microscopy. To quantify penetration of cellophane membranes, conidia were inoculated onto autoclaved Visking dialysis tubing (Carl Roth GmbH, Karlsruhe, Germany) and observed by phase-contrast microscopy. Appressorium turgor was assessed using a cell collapse (cytorrhysis) assay. Appressoria formed after 24 h on polystyrene Petri dishes were treated for 10 min with 0, 100, 200, 300, 400 or 500 mg ml^{-1} PEG6000 and *c.* 300 appressoria per treatment were scored for collapse by microscopy. For simultaneous cytochemical localization of ChELP2 and chitin on fungal infection structures, infected leaf epidermis was peeled off and labelled sequentially with MAb UB25, goat antimouse secondary antibody conjugated with fluorescein isothiocyanate (FITC), and wheat germ agglutinin (WGA) conjugated with tetramethylrhodamine isothiocyanate (TRITC) (Perfect *et al.*, 2000). Labelled samples were viewed with either Leica TCS SP2 or Zeiss LSM 700 confocal laser scanning microscopes. For imaging FITC fluorescence, excitation was at 488 nm and emission was detected at 490–555 nm. For imaging TRITC fluorescence, excitation was at 555 nm and emission was detected at 557–600 nm.

Transmission electron microscopy and lectin cytochemistry

For ultrastructural localization of chitin, samples of infected leaf tissue (3 d postinoculation) were cryofixed by high-pressure freezing, freeze-substituted in acetone and embedded in acrylic resin (Micali *et al.*, 2011). Ultrathin sections were labelled with WGA conjugated to 10 nm colloidal gold particles (EY Laboratories, San Mateo, CA, USA), as described previously (O'Connell & Ride, 1990). For transmission electron microscopy (TEM) analysis of appressoria, infected cotyledons (24 hpi) were fixed in 2.5% (v/v) glutaraldehyde and 2% (w/v) paraformaldehyde in 0.05 M sodium cacodylate buffer (pH 6.9), followed by postfixation on ice for 1 h in 0.5% (w/v) osmium tetroxide and 0.15% (w/v) potassium ferricyanide in the same buffer. After dehydration in ethanol, samples were embedded in epoxy resin (Araldite 502/Embed 812; Electron Microscopy Services, Hatfield, PA, USA). Sections were stained with 0.1% (w/v) potassium permanganate in 0.1 N sulphuric acid for 1 min (Sawaguchi *et al.*, 2001) before imaging with a Hitachi H-7650 TEM (Hitachi High-Technologies Europe GmbH, Krefeld, Germany) operating at 100 kV.

Chitin-binding assays

The glycan array (version 4.2) used here contains 511 natural and synthetic glycans representing major glycan structures of glycoproteins and glycolipids (Blixt *et al.*, 2004; http://www.functionalglycomics.org/static/consortium/resources/resourcecoreh15.shtml). The binding of FLAG-tagged recombinant ChELP1 and ChELP2 (200 μg ml^{-1}) to the array was detected by immunofluorescence using anti-FLAG monoclonal antibodies and FITC-conjugated secondary antibodies, as described by Al Atalah *et al.* (2011). After removing the highest and lowest values among six replicates, average relative fluorescence was calculated

for each glycan. Polysaccharide affinity precipitation assays were carried out as described previously (van den Burg *et al.*, 2006) using 200 µg ml^{-1} ChELP1 and ChELP2 with chitin beads (New England Biolabs, Beverly, MA, USA), crab shell chitin, chitosan, xylan or cellulose. The binding affinities of ChELP1 and ChELP2 for chitin oligosaccharides were measured by surface plasmon resonance using a Biacore X100 instrument (GE Healthcare UK Ltd, Little Chalfont, UK), with biotinylated chitin oligosaccharide ((GlcNAc)$_8$-Bio) immobilized on the sensor tip (Mentlak *et al.*, 2012).

Fungal chitin samples were prepared by chemical digestion of *C. higginsianum* spore walls based on the method of Gow *et al.* (1980). Briefly, spores were boiled in 5% KOH for 30 min, rinsed in water, autoclaved in 1 : 1 glacial acetic acid : 30% H$_2$O$_2$ for 15 min and rinsed in water. After further boiling in 5% KOH, the spores were rinsed in water and dried onto poly-L-lysine-coated multiwell slides. The chitin-enriched walls were incubated for 1 h with either recombinant ChELP (100 µg ml^{-1}) or ChELP preincubated for 1 h with chitin hydrolysate (1 : 10 dilution; Vector Laboratories, Burlingame, CA, USA). Binding of the ChELPs was detected by immunofluorescence using anti-FLAG antibodies (1 : 1000) and FITC-conjugated goat antimouse antibodies (1 : 50) and viewed with confocal microscopy.

Chitinase inhibition assay

A crude extract of tomato leaves containing chitinases was prepared as described previously (Joosten *et al.*, 1995). Aliquots (40 µl) of *Trichoderma viride* spore suspension (10^4 conidia ml^{-1}) were allowed to germinate overnight, and incubated with either ChELP1 or ChELP2 recombinant proteins (30 µM). After 2 h, an extract of tomato hydrolytic enzymes (5 µl) was added and the spores were visualized 4 h later. The recombinant proteins Avr4 and Ecp6 were used as positive and negative controls, respectively (van den Burg *et al.*, 2006; de Jonge *et al.*, 2010).

Chitin-induced medium alkalinization assay

The assay was performed as described previously (de Jonge *et al.*, 2010) using either recombinant ChELP1 or ChELP2. After treating tomato suspension cultured cells with 10 nM chitin hexamer ((GlcNAc)$_6$), 100 nM recombinant protein or both components together, the pH of the medium was monitored continuously using a glass electrode.

Mitogen-activated protein kinase (MAPK) activation assay

Arabidopsis Col-0 seedlings were grown hydroponically for 2 wk in half-strength Murashige and Skoog liquid medium. Chitin heptamer ((GlcNAc)$_7$) (1 µM; Elicityl SA, Crolles, France) was preincubated with or without recombinant ChELP1 or ChELP2 (10 µM) for 1 h at room temperature before application to the seedlings. MAPK assays were performed as described by Tsuda *et al.* (2009) with minor modifications. Briefly, equal amounts of protein from crude plant extracts were separated by SDS-PAGE

in 10% polyacrylamide gels, transferred to nitrocellulose membranes and probed with phospho-p44/p42 MAPK primary antibodies followed by horseradish peroxidase-tagged goat antirabbit secondary antibodies (Cell Signaling Technology, Leiden, the Netherlands).

RNAi-mediated gene silencing of ChELP1

The C-terminal 246 bp of the *ChELP1* coding region, including LysM domains, was fused to the TrpC promoter and terminator and ligated into binary vector pBIG4MRH containing the hygromycin resistance gene as a selectable maker for fungal transformants. The vector, designated pBIG4_AS_CIH1, was introduced into *Agrobacterium tumefaciens* and transformed into *C. higginsianum* as described by Huser *et al.* (2009). For assessment of disease symptoms, RT-qPCR analysis of fungal biomass and microscopic evaluation of appressorial penetration frequency, three independent transformants were inoculated on 4-wk-old *Arabidopsis* plants (Takahara *et al.*, 2009) and compared with the wild-type.

Results

C. higginsianum encodes a large and diverse arsenal of putative LysM effectors

Previously, 22 proteins harbouring at least one CBM50 (LysM) module were identified in *C. higginsianum* (O'Connell *et al.*, 2012). After manual curation, we found five genes were split between contigs, giving a total of 18 LysM domain proteins (Table S2). Among these proteins, six were not predicted to be secreted. These include five hypothetical proteins and a protein (CH063_05984) with predicted Cyanovirin-N homolog and Rick (*Rickettsia* 17 kDa surface antigen) domains that resembles a nonsecreted LysM protein previously reported from *M. oryzae* (Koharudin *et al.*, 2011). The 12 remaining LysM proteins were predicted to be extracellular, including two chitinases containing the glycoside hydrolase 18 catalytic domain. In order to identify *C. higginsianum* effectors that could interfere with plant immune responses, we excluded chitinases and focused on the 10 remaining ChELPs without predicted enzymatic domains (Fig. 1a). The size of these proteins ranges between 82 and 595 residues (ChELP3 and ChELP10, respectively) and they harbour from one to six LysM domains.

ChELP-encoding genes are strongly induced *in planta*

In order to profile the expression of *ChELP* genes during infection, we used RNA sequencing data obtained from *C. higginsianum* appressoria formed *in vitro* (VA, 22 hpi) and infected *Arabidopsis* leaves corresponding to prepenetration appressoria (PA, 22 hpi), the early biotrophic phase (BP, 40 hpi) and the transition from biotrophy to necrotrophy (NP, 60 hpi) (O'Connell *et al.*, 2012) (Fig. 1b). Transcripts of *ChELP8*, *ChELP9* and *ChELP10* were barely detected in the four conditions tested (read counts < 5; Table S2). Strikingly, all the
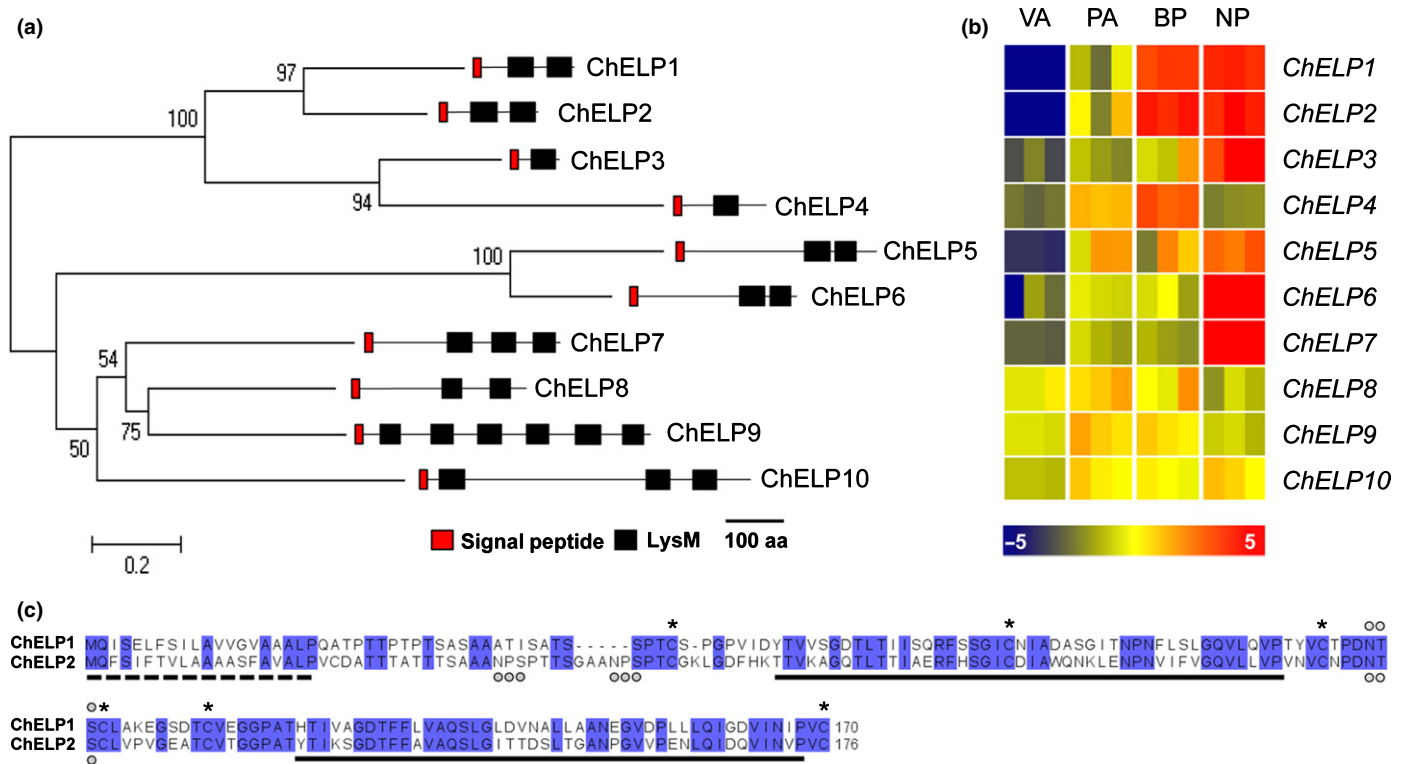
Fig. 1 Phylogeny, structure and gene expression of *Colletotrichum higginsianum* extracellular LysM proteins (ChELPs). (a) Phylogeny of ChELPs. The phylogram was constructed based on a multiple alignment of full-length amino acid sequences using CLUSTALW. The resulting alignment was then used to generate a neighbour-joining tree with MEGA4.1 using the following parameters (pairwise deletion, amino: Poisson correlation). Scale: amino acid substitutions per site. The protein domain organization depicted on the right side of the tree was predicted using the pfam database (http://pfam.xfam. org/). (b) Expression profiling of *ChELPs* measured using RNA sequencing. Overrepresented (dark red) or underrepresented transcripts (dark blue) are depicted as $\log_2$ fold-changes relative to the mean expression measured across all four stages selected for RNA sequencing, namely: *in vitro* appressoria (VA; 22 h postinoculation (hpi)); *in planta* appressoria (PA; prepenetration, 22 hpi); biotrophic phase (BP; 40 hpi); and necrotrophic phase (NP; 60 hpi). (c) Sequence similarities between ChELP1 and ChELP2. Full-length protein sequences were aligned using CLUSTALW and the alignment was edited using JALVIEW (http://www.jalview.org/). Solid black bars represent LysM domains, dashed bars indicate predicted signal peptides. Conserved cysteine residues are highlighted with an asterisk and potential N-glycosylation sites with circles.

remaining expressed *ChELPs* were induced after fungal penetration into host cells; thus *ChELP3*, *ChELP5*, *ChELP6* and *ChELP7* transcripts were preferentially detected at the transition to necrotrophy, whereas an earlier accumulation concomitant with the biotrophic phase was observed for *ChELP1*, *ChELP2* and *ChELP4* (Fig. 1b). *ChELP1* and *ChELP2* were selected for functional characterization because they were the most highly expressed of all the *ChELP* genes (read counts > 1000; Table S2), suggesting that they could play important roles during early pathogenesis.

ChELP1 and ChELP2 are not lineage-specific innovations

Colletotrichum higginsianum extracellular LysM protein 1 and ChELP2 are paralogues that share 50% amino acid identity, including six conserved cysteine residues, which may be involved in the formation of disulphide bonds (Fig. 1c). Potential *N*-glycosylation sites were detected in both proteins. ChELP1 and ChELP2 share sequence similarities with secreted LysM effectors previously characterized from other ascomycetes (Fig. S1a,b). Phylogeny analysis revealed that ChELP1 is most closely related to the *M. oryzae* Slp1 effector (Mentlak *et al.*, 2012), whereas ChELP2 is

more similar to CgELP2 of *Colletotrichum graminicola* and CIH1 of *Colletotrichum lindemuthianum* (Perfect *et al.*, 1998). ChELP1 and ChELP2 also resemble *C. fulvum* Ecp6 except that the C-terminal part of Ecp6 is longer and contains a third LysM domain (Fig. S1b). Modelling of ChELP1 and ChELP2 onto the previously resolved ternary structure of Ecp6 (Sánchez-Vallet *et al.*, 2013) revealed a flexible loop between the two LysM domains, similar to Ecp6 (Fig. S1c).

ChELP1 and *ChELP2* are preferentially transcribed during biotrophy and their products accumulate at the plant–fungal interface

To confirm the expression patterns of *ChELP1* and *ChELP2* measured by RNA-Seq (Fig. 1b) and to monitor their expression dynamics with finer resolution, we analysed three fungal developmental stages *in vitro* (dormant spores, vegetative mycelium and mature appressoria) and four *in planta* stages (prepenetration appressoria, the early biotrophic phase, the switch to necrotrophy and the late necrotrophic stage) using RT-qPCR (Fig. 2a,b). The expression of both *ChELP1* and *ChELP2* was strongly induced *in planta* during the early biotrophic phase and, to a lesser extent, at

the switch to necrotrophy. However, both genes were also transcribed at basal levels in vegetative mycelium and appressoria *in vitro* and *in planta*.

To localize ChELP2 protein *in planta*, we used MAb UB25, which recognizes a protein epitope in the *C. lindemuthianum* LysM protein CIH1 (Pain *et al.*, 1994). In western blots, UB25 bound ChELP2 but not ChELP1 (Fig. S2a), consistent with the greater protein sequence identity of CIH1 to ChELP2 (49%) than to ChELP1 (42%). In SDS-PAGE gels (Fig. S2a,b), *Pichia*-expressed ChELP1 and ChELP2 displayed an apparent Mr (~ 29 kDa) larger than that predicted from their protein sequences (17.1 and 18 kDa, respectively), suggesting they may be glycosylated. Consistent with this, both proteins stained with periodic acid–Schiff reagent (Fig. S2b), while periodate oxidation and β-elimination experiments suggested the presence of *N*-linked mannose sidechains (Fig. S2c).

UB25 antibodies did not label the external surfaces of spores, germ tubes or appressoria, but the bulbous, biotrophic primary hyphae were intensely labelled at all stages of their development inside host epidermal cells, including young hyphae formed immediately after penetration (Fig. 3a,b). The fluorescence was not uniformly distributed over the fungal cell surface but instead was concentrated in small punctate structures. These were smaller and more numerous than the interfacial bodies that are foci for the accumulation of other *C. higginsianum* effectors (Kleemann *et al.*, 2012). After the switch to necrotrophy, the filamentous secondary hyphae were not labelled by UB25, with an abrupt transition in surface labelling occurring at the point where secondary hyphae emerged from the primary hyphae (Fig. 3c). We also used
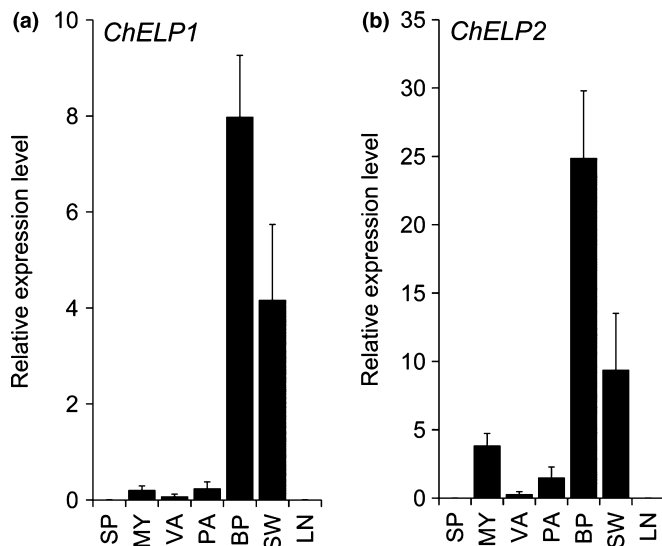
the lectin WGA to compare the distribution of chitin on fungal infection structures. Although chitin was abundantly exposed on the surface of necrotrophic secondary hyphae, it was not detectable on biotrophic primary hyphae (Fig. 3c,d). Nevertheless, cell walls of primary hyphae were strongly labelled by WGA in cross-sections (Fig. 3e), suggesting that chitin is present in the walls of biotrophic hyphae but is not accessible at the hyphal surface because of masking by other wall components. Simultaneous localization of chitin and ChELP2 confirmed a strong correlation between presence of the LysM effector and inaccessibility of chitin to WGA (Fig. 3).

ChELP1 and ChELP2 bind chitin polymer and oligomers *in vitro*

One of the key features of fungal LysM effectors is their ability to bind chitin (de Jonge & Thomma, 2009). To determine which glycan(s) are bound by ChELP1 and ChELP2 *in vitro*, we used *Pichia*-expressed recombinant proteins to screen a glycan array comprising 511 glycans. ChELP1 and ChELP2 showed a similar binding pattern that was confined to only three glycans (numbers 185, 186 and 187) corresponding to chitin oligomers of varying length, namely chitotriose $(GlcNAc)_3$, chitopentaose $(GlcNAc)_5$ and chitohexaose $(GlcNAc)_6$ (Fig. 4a; Table S3). To examine the affinity of the ChELPs for chitin oligomers in more detail, we used surface plasmon resonance with the ligand $(GlcNAc)_8$ immobilized on the sensor chip. In this assay, ChELP1 showed greater affinity for chitin oligomers than ChELP2, with dissociation constants (K_d values) of 2.6×10^{-11} and 2.5×10^{-10} M, respectively (means of two independent experiments, data not shown). Using similar methods, the binding affinities of *C. fulvum* Ecp6 and *M. oryzae* Slp1 were previously found to be lower ($K_d = 1.3 \times 10^{-9}$ and 2.4×10^{-9} M, respectively) (Mentlak *et al.*, 2012). Overall, these results suggest that ChELP1 and ChELP2 both possess high affinity for chitin oligomers.

In addition to chitin oligosaccharides, both ChELP1 and ChELP2 were able to bind chitin polymer, in the form of crab shell chitin or shrimp shell-derived chitin beads. However, they did not bind to chitosan (deacetylated chitin) or the plant cell wall polymers xylan and cellulose, confirming that both proteins are specific for chitin (Fig. 4b). To verify the ability of ChELPs to bind fungal cell wall chitin, we first used chemical digestion to make chitin more accessible by removing proteins, glucans and mannans from spore walls. We then used immunofluorescence to detect the binding of recombinant ChELPs to these thin cell wall envelopes. Both proteins strongly labelled spore walls, but binding was abolished when the proteins were preincubated for 1 h with chitin hydrolysate (Fig. 4c), confirming that ChELP1 and ChELP2 specifically bind cell wall chitin.

ChELP1 and ChELP2 do not protect fungal hyphae against plant chitinases

It was previously reported that some chitin-binding effectors can protect fungal cell walls against hydrolysis by plant chitinases (van den Burg *et al.*, 2006; Marshall *et al.*, 2011). To determine
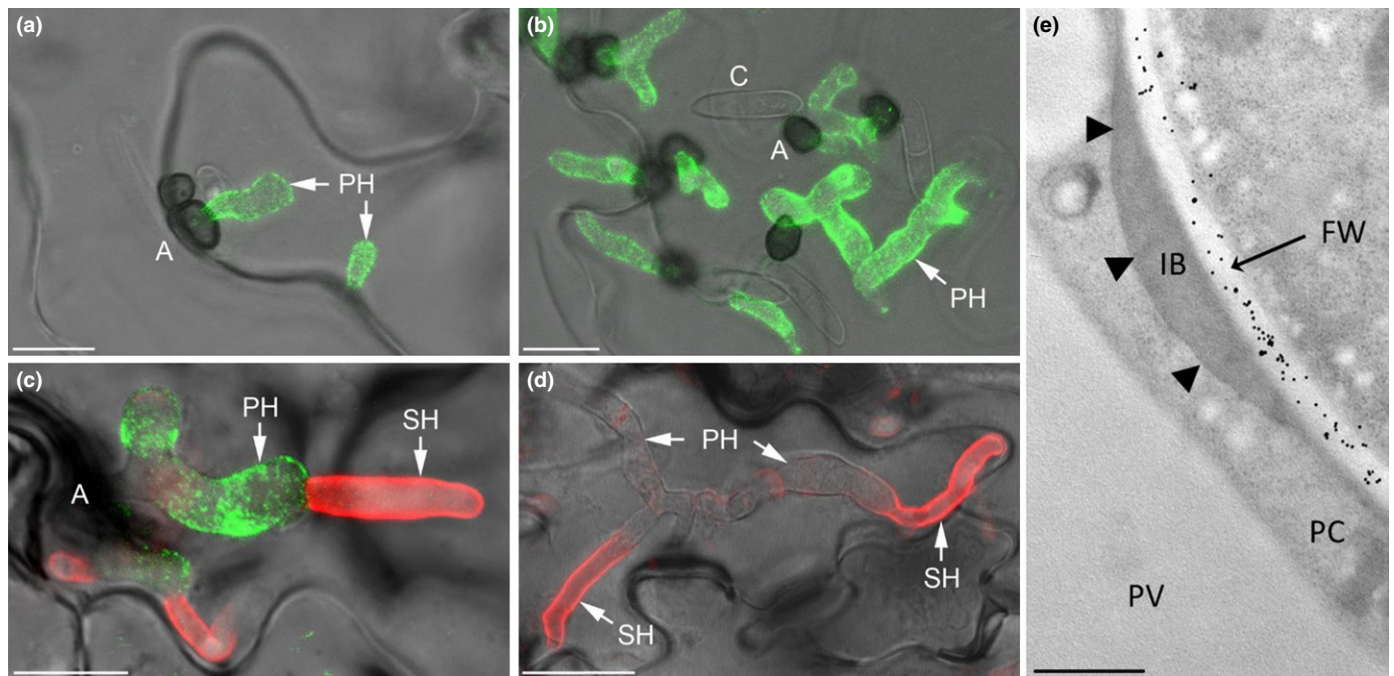

Fig. 2 *ChELP1* and *ChELP2* are biotrophy-associated genes. Expression profiling of (a) *ChELP1* and (b) *ChELP2* genes was assessed using reverse transcription quantitative polymerase chain reaction and expression levels are shown relative to the mean expression of the two *Colletotrichum higginsianum* reference genes Actin and α-Tubulin. *In vitro* cell types are dormant spores (SP), vegetative mycelium (MY) and mature appressoria (VA). *In planta* stages are mature appressoria (PA), early biotrophic phase (BP), biotrophy to necrotrophy switch (SW) and late necrotrophy (LN). Error bars = 1 SD ($n = 3$).

Fig. 3 *Colletotrichum higginsianum* extracellular LysM protein 2 (ChELP2) is localized at the biotrophic interface. (a–d) Confocal micrographs showing the localization of ChELP2 and chitin in *C. higginsianum*-infected *Arabidopsis* leaf tissue after immunofluorescence labelling with monoclonal antibody UB25 (green) and wheatgerm agglutinin (WGA, red), respectively. Double labelling with both probes is illustrated in (c). (a–c) UB25 detects ChELP2 only on the surface of biotrophic primary hyphae (PH), not on conidia (C), appressoria (A) or necrotrophic secondary hyphae (SH). (c, d) WGA detects chitin on secondary hyphae, but not primary hyphae. Bars, 10 μm. (e) Transmission electron micrograph showing a cross-section through part of a biotrophic primary hypha. Chitin is detected in the fungal wall (FW) by labelling with WGA conjugated to colloidal gold particles, but is not detected in the interfacial body (IB). The invaginated plant plasma membrane is indicated with arrowheads. PC, plant cytoplasm; PV, plant vacuole. Bar, 500 nm.

whether ChELP1 and ChELP2 have this ability, we used a method based on growth inhibition of *Trichoderma viride* germ tubes by tomato chitinases (van den Burg *et al.*, 2006). *T. viride* spores were incubated for 2 h with either ChELP1 or ChELP2, followed by the addition of tomato leaf extract containing basic vacuolar chitinases. Similar to *C. fulvum* Ecp6, but unlike *C. fulvum* Avr4, ChELP1 and ChELP2 do not protect *Trichoderma* cell walls from the deleterious effects of plant chitinases (Fig. S3).

ChELP1 and ChELP2 suppress chitin-triggered plant immune responses

To test whether ChELP1 and ChELP2 interfere with plant immune responses by preventing host recognition of fungal chitin fragments (de Jonge & Thomma, 2009), we treated *A. thaliana* seedlings grown in liquid culture with chitin hep-tamer (($GlcNAc)_7$) and monitored the activation of defence-related MAPKs using immunoblotting (Tsuda *et al.*, 2009). Rapid phosphorylation of MPK3 and MPK6 began 2.5 min after application of 1 μM $(GlcNAc)_7$, increasing to a maximum by 5 min (Fig. 5). By contrast, preincubation of the chitin fragments for 1 h with 10 μM ChELP1 (Fig. 5a), and to a lesser extent ChELP2 (Fig. 5b), reduced MAPK activation, suggesting that both proteins can suppress chitin-triggered immune responses by sequestering chitin. Treatment with ChELP proteins alone induced only weak MAPK activation (Fig. 5a,b). These

experiments were repeated three times with similar results (data not shown). To verify these findings in an independent assay, we used tomato suspension-cultured cells elicited with chitin hex-amer $(GlcNAc)_6$ (Fig. S4). Chitin-induced defense activation is indicated by a pH shift leading to medium alkalinization (Felix *et al.*, 1993). Treatment of the cells with 10 nM of chitin hex-amer caused medium alkalinization. However, simultaneous addition of 100 nM of ChELP1 protein to the medium strongly attenuated this alkaline pH shift, indicating that ChELP1 can suppress chitin-induced immune responses not only in *Arabidopsis* but also in tomato (Fig. S4a). Similar results were observed using lower concentrations of chitin hexamers and ChELP1 protein (1 nM and 10 nM respectively, data not shown). However, ChELP2 alone induced a strong and delayed pH shift in the absence of exogenous chitin hexamer (Fig. S4b), suggesting the protein may be recognized by tomato cells.

ChELP1 and ChELP2 are required for virulence and establishment of biotrophy

We attempted to test the contribution of *ChELP1* and *ChELP2* to fungal virulence by targeted gene disruption using *A. tumefaciens*-mediated transformation (ATMT). However, tar-geted mutants were not obtained, possibly because the genes are located in genomic regions recalcitrant to T-DNA insertion. We therefore used RNAi-mediated gene silencing coupled with ATMT to generate *C. higginsianum* mutants in which an
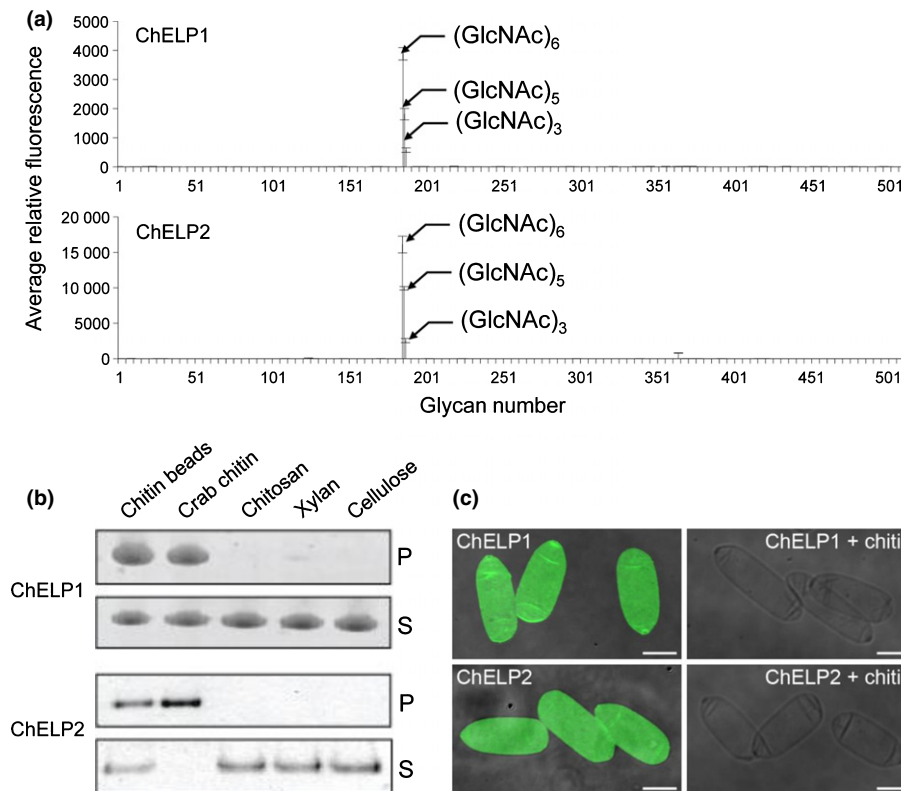
Fig. 4 *Colletotrichum higginsianum* extracellular LysM proteins 1 and 2 (ChELP1 and ChELP2) bind specifically to chitin and chitin oligomers. (a) Screening of glycan-binding specificities of ChELP1 and ChELP2 recombinant proteins using a printed glycan array. The array contains a library of 511 natural and synthetic glycan sequences (see Supporting Information Table S3 for identities). Average relative fluorescence intensities measured after immunodetection of ChELP1 (top) and ChELP2 (bottom) are presented. ChELP1 and ChELP2 only hybridize to probe numbers 185, 186 and 187 corresponding to chitin oligomers $(GlcNAc)_6$, $(GlcNAc)_5$, and $(GlcNAc)_3$, respectively. Fluorescence intensities are higher for ChELP2, suggesting a higher binding affinity than ChELP1. (b) Affinity precipitation of ChELP1 and ChELP2 in the presence of the following insoluble carbohydrates: chitin beads, crab shell chitin, chitosan, xylan and cellulose. Following centrifugation, both the supernatant (S) and the pellet (P) samples were analysed. Detection of ChELP1 and ChELP2 in the pellet fraction indicates specific binding to chitin and crab shell chitin only. (c) Binding of ChELP1 and ChELP2 to fungal cell wall chitin. *C. higginsianum* spores were chemically extracted to remove proteins, glucans and mannans, leaving thin cell wall envelopes composed largely of chitin. Binding of recombinant ChELP1 and ChELP2 proteins to fungal chitin (left) was detected by immunofluorescence. Preincubation of the proteins with chitin hydrolysate (right) abolished labelling. Images were collected by confocal microscopy using identical exposure settings. Bars, 10 μm.

antisense version of the LysM domains of *ChELP1* was expressed from a strong constitutive promoter (Fig. S5a). Silencing of *ChELP1* did not affect mycelial growth *in vitro* (Fig. S5b) but strongly reduced the ability of *C. higginsianum* to infect *Arabidopsis* plants, as shown by the less severe disease symptoms produced by the three silencing mutants (T2, T3, T4) compared with the wild-type (Fig. 6a). To confirm that *ChELP1* transcript accumulation was attenuated in the silencing mutants, we performed RT-qPCR using cDNA derived from 5-d-old mycelium. We found a significant reduction in transcript abundance not only for *ChELP1* (10-fold compared with the wild-type) but also for its paralogue *ChELP2* (fourfold reduction compared with the wild-type) (Fig. S6). This probably reflects the relatively high sequence identity (73%) between the 246 bp silencing construct and the C-terminal portion of the ChELP2 transcript (Fig. S5c). Expression levels for the control genes *ChG6PDH*, *ChElF* and *ChEMP1* were similar in the wild-type and silencing mutants (Fig. S6). Thus, the reduced virulence of the mutants is likely to result from silencing both *ChELP1* and *ChELP2*.

To precisely monitor differences in fungal biomass between the RNAi mutants and the wild-type during infection, the *C. higginsianum* actin DNA fragment was amplified by qPCR, using the *Arabidopsis* actin gene for normalization. A massive reduction in the amount of fungal actin DNA was observed at 84 hpi for the silencing mutants, representing a 50-fold reduction in fungal biomass compared with the wild-type (Fig. 6b). Microscopic evaluation of appressorial penetration frequency at 84 hpi revealed that only 0.4–1.8% of appressoria from the silencing mutants were able to penetrate host epidermal cells and form visible biotrophic primary hyphae, compared with 53% for the wild-type (Fig. 6c). In those cases where penetration was successful, subsequent growth of the primary hyphae was highly restricted and necrotrophic secondary hyphae were rarely observed (Fig. 6d). Taken together, these results suggest that ChELP1 and ChELP2 are essential for successful host cell penetration and establishment of intracellular biotrophic hyphae.

Virulence of *ChELP1* RNAi mutants is not restored on plant chitin receptor mutants

In *Arabidopsis*, chitin recognition is mediated by at least two plasma membrane pattern recognition receptors, namely CERK1
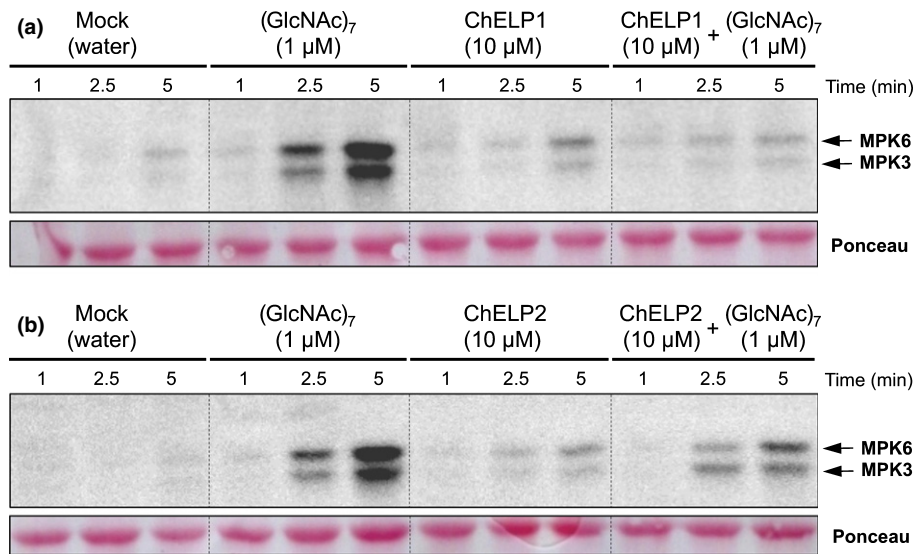
Fig. 5 *Colletotrichum higginsianum* extracellular LysM proteins 1 and 2 (ChELP1 and ChELP2) suppress chitin-induced activation of *Arabidopsis* immunity-related mitogen-activated protein kinases MAPKs. Western blot analysis of *Arabidopsis thaliana* Col-0 seedlings at the indicated time points after treatment with 1 μM chitin heptamer (GlcNAc)$_7$ with or without 10 μM ChELP1 (a) or 10 μM ChELP2 (b). Activated MAPKs were detected by probing the blots with anti-p44/42 MAPK antibodies. Ponceau S stained blots showing the RuBisCO large subunit indicate equal protein loading. Control plants were treated with water only (mock), ChELP1 only or ChELP2 only. ChELP1, and to a lesser extent ChELP2, suppresses chitin-induced phosphorylation of MPK3 and MPK6. Experiments were conducted three times with similar results.

and the CEBiP homolog LYM2, which operate through independent signalling pathways to confer resistance to fungal pathogens (Miya *et al.*, 2007; Shinya *et al.*, 2012; Faulkner *et al.*, 2013). We hypothesized that if ChELP1 and ChELP2 interfere with plant chitin perception, the virulence of the RNAi mutants should be restored or enhanced on plants lacking CERK1 or LYM2. We therefore evaluated appressorial penetration frequency of the *ChELP1* RNAi mutants on *Arabidopsis cerk1-2* and *lym2-1* single mutants and the *lym1-1 lym2-1 lym3-1* triple mutant. We found no significant increase in fungal entry rate on any of the mutants compared with Col-0 wild-type plants (Fig. 7a). Similarly, penetration by wild-type *C. higginsianum* was not significantly enhanced on any of the plant mutants.

ChELP1 RNAi mutants are impaired in appressorial function and display morphological abnormalities

Given the very low frequency of host cell penetration by the *ChELP1* RNAi mutants, we checked whether their appressoria were still able to penetrate artificial cellophane membranes. Wild-type *C. higginsianum* appressoria penetrated cellophane with high frequency (mean = 96.2%, Fig. 7b), forming hyphae inside the membrane (see Kleemann *et al.*, 2012). In striking contrast, < 1% of appressoria of the three silencing mutants were able to penetrate cellophane (Fig. 7b). Moreover, the mutant germlings showed a variety of morphological abnormalities. Thus, whereas wild-type spores germinated on cellophane to form a single unbranched germ tube subtending a single appressorium (Fig. 7c), spores of the RNAi mutants sometimes produced two germ tubes and two appressoria (Fig. 7d), or a bifurcated germ tube with two appressoria (Fig. 7e). In addition, secondary germ tubes emerged laterally from 8% to 29% of

mutant appressoria and thereafter grew over the cellophane surface (Fig. 7f). The frequency of these abnormalities is quantified in Fig. 7(g) and (h). To test whether appressoria of the RNAi mutants were affected in turgor generation, we conducted plasmolysis/cytorrhysis assays with a range of osmolyte concentrations (Howard *et al.*, 1991). No difference in turgor was detected between wild-type and mutant appressoria at 24 h (Fig. S7), indicating that the penetration defect of the mutants is not a result of reduced turgor. Finally, using TEM to examine appressoria formed on cotyledons, we found mutant and wild-type appressoria were indistinguishable in their ultrastructure, and the penetration pore and surrounding wall layers appeared normal in the mutants (Fig. S8). Taken together, our results indicate that silencing *ChELP1* and *ChELP2* impairs the penetration ability of appressoria in a plant-independent manner, which probably explains why fungal virulence was not restored on the plant chitin-receptor mutants.

Discussion

The first extracellular LysM domain protein to be identified in any fungus was CIH1 from *C. lindemuthianum*, which was detected in the cell walls of biotrophic hyphae infecting bean (Pain *et al.*, 1994; Perfect *et al.*, 1998). The presence of tandem LysM domains was noted, but *CIH1* targeted replacement mutants retained full pathogenicity, possibly as a result of functional redundancy (Perfect *et al.*, 2000). Thus, no information was available on the role of LysM effectors in the economically important genus *Colletotrichum*. More recently, genome sequencing revealed that LysM domain-containing proteins are dramatically expanded in *Colletotrichum* species (20 in *C. gloeosporioides*, 18 in *C. higginsianum*, 14 in *C. graminicola* and 12 in
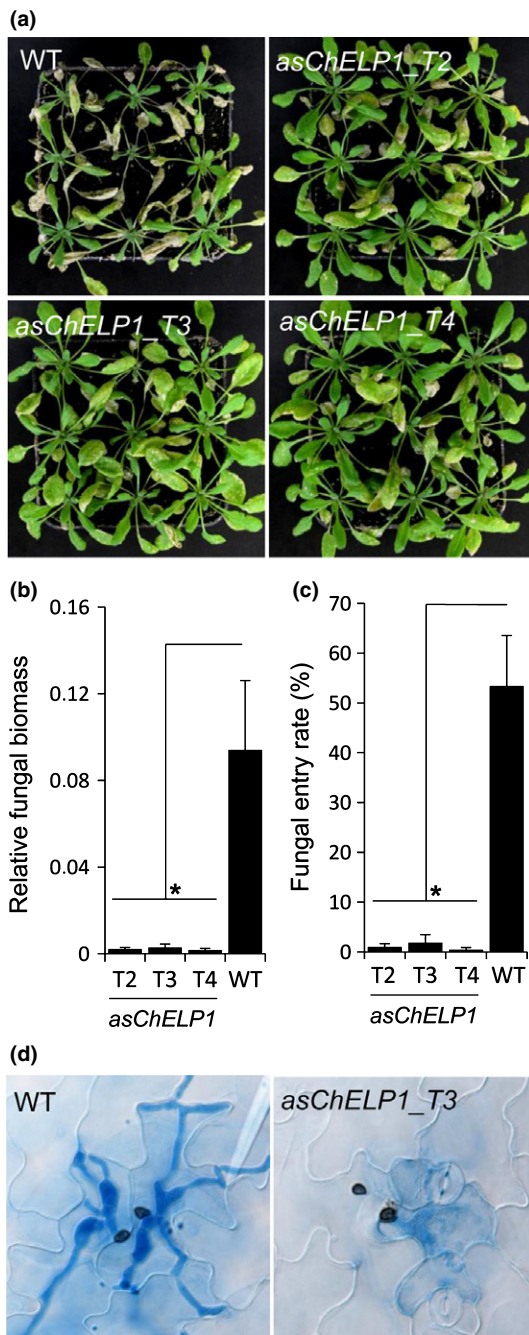
Fig. 6 *Colletotrichum higginsianum* extracellular LysM protein 1 (ChELP1) is a virulence effector required for anthracnose disease. (a) Disease symptoms on *Arabidopsis thaliana* Col-0 leaves infected with the *C. higginsianum* wild-type strain (WT) or three independent transformants (T2, T3, T4) in which *ChELP1* expression was suppressed by RNAi-mediated gene silencing. Pictures were taken 6 d postinoculation (dpi). (b) Fungal biomass during infection was monitored by quantitative PCR after amplification of the *C. higginsianum* Actin DNA gene fragment relative to the *A. thaliana* Actin2 DNA gene fragment. Total DNA was extracted from leaf tissues inoculated either with *C. higginsianum* WT strain or three silencing mutants at 84 h postinoculation (hpi). Asterisk indicates significant differences (*t*-test, $P < 0.05$). Error bars = 1 SE ($n = 3$). (c) Histogram showing the frequency of appressorial penetration by the WT strain and three silencing mutants (T2, T3, T4) into *Arabidopsis* epidermal cells at 3 dpi. Data represent mean counts based on at least 100 appressoria for each of three biological replicates. Asterisks indicate significant differences (*t*-test, $P < 0.05$). Error bars = 1 SD. (d) Light micrographs showing *Arabidopsis* leaf tissue stained with lactophenol-Trypan blue at 3 dpi. Appressoria of the WT strain penetrate and form primary and secondary hyphae, whereas those of *ChELP1* silencing transformant T3 either fail to penetrate or form primary hyphae confined to one host cell.

genome of the root endophytes *Piriformospora indica* (Zuccaro *et al.*, 2011; Rafiqi *et al.*, 2013) and *Colletotrichum tofieldiae* (Hacquard *et al.* 2016), suggesting potential evolutionary convergence in the sequestration of chitin fragments between beneficial root endophytic fungi and leaf-associated pathogenic fungi.

Consistent with the presence of two LysM domains in ChELP1 and ChELP2, the recombinant proteins bound specifically to chitin oligomers in a glycoarray of 511 glycans, and in surface plasmon resonance assays they bound chitin octamer with higher affinity than reported previously for *C. fulvum* Ecp6 and *M. oryzae* Slp1 (Mentlak *et al.*, 2012). In addition to chitin oligosaccharides, recombinant ChELP1 and ChELP2 also bound chitin polymer from crustacean shells as well as fungal cell wall chitin. Recent analysis of the crystal structure of Ecp6 revealed that two of the three LysM domains in this protein dimerize to provide a single chitin-binding pocket with ultrahigh affinity. This binding pocket may outcompete plant chitin receptors that bind chitin via a single LysM domain with much lower affinity (Sánchez-Vallet *et al.*, 2013). The striking structural similarities between Ecp6, ChELP1 and ChELP2, including the orientation of their chitin-binding sites and the presence of a flexible loop between the two LysM domains in both ChELPs, suggest these domains could similarly dimerize to provide a high-affinity chitin-binding pocket.

When expressed by *Pichia*, ChELP1 and ChELP2 displayed molecular weights in SDS-PAGE gels *c.* 60% higher than predicted from their protein sequences, suggesting they are subject to posttranslational modification. Each protein has two to three predicted *N*-glycosylation sites, and the *Pichia*-expressed proteins are mannosylated. Thus, both ChELP1 and ChELP2 are likely to contain *N*-linked glycans, although the presence of *O*-linked glycosylation cannot be excluded. The potential importance of glycosylation was highlighted by a recent study on *M. oryzae* Slp1, where *N*-glycosylation is critical for the chitin-binding activity and virulence function of the protein (Chen *et al.*, 2014).

C. orbiculare), surpassing most other basidiomycete and ascomycete fungal pathogens sequenced so far (O'Connell *et al.*, 2012; Gan *et al.*, 2013). The majority of these are secreted proteins without chitinase enzymatic domains, suggesting a role as effectors for chitin sequestration and evasion of host immune responses. Similar to *ChELP1* and *ChELP2*, *C. lindemuthianum CIH1* and its closest homologues in *C. graminicola* (GLRG_02947) and *C. orbiculare* (Cob_07509) all show peak expression during biotrophic infection of bean, maize and *Nicotiana*, respectively (O'Connell *et al.*, 2012; Gan *et al.*, 2013), suggesting that deployment of such effectors is a hallmark of intracellular biotrophy in this fungal genus. Interestingly, an expansion of secreted LysM proteins (23) was also found in the
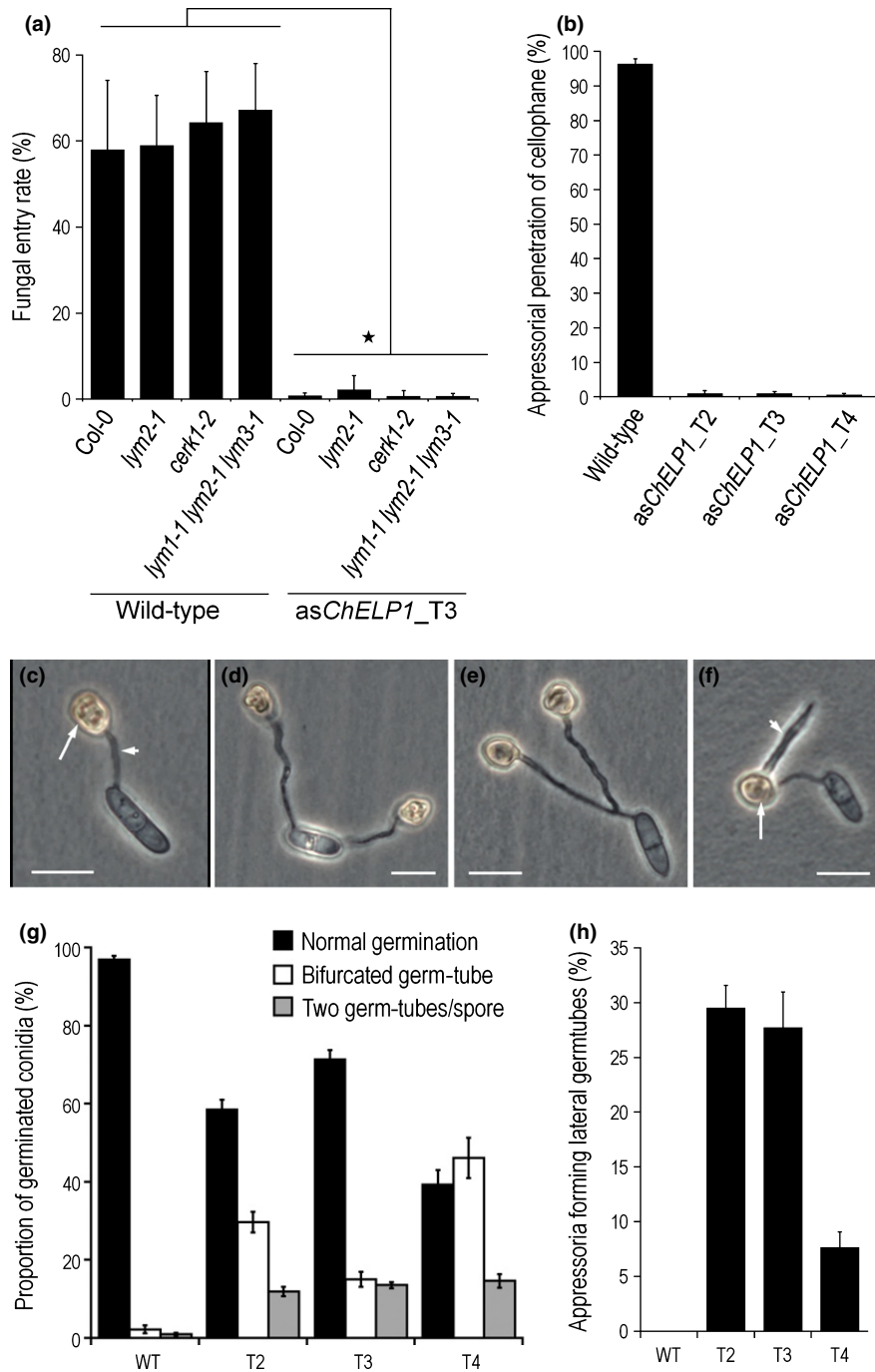
Fig. 7 Appressoria of *ChELP1* RNAi mutants fail to penetrate *Arabidopsis* epidermal cells and cellophane membranes *in vitro*. (a) Histogram showing the frequency of penetration by appressoria of the *Colletotrichum higginsianum* wild-type (WT) strain and *ChELP1* RNAi transformant T3 into epidermal cells of *Arabidopsis* Col-0, *cerk1-2* and *lym2-1* single mutants and the *lym1-1 lym2-1 lym3-1* triple mutant (all in the Col-0 background) at 3 d postinoculation (dpi). Data are mean percentages based on > 100 appressoria from each of three leaves per replicate, three replicates per fungal/plant combination. Asterisk indicates significant differences (*t*-test, *P* < 0.05). Error bars = 1 SD. (b) Histogram showing the appressorial penetration frequency of the wild-type and *ChELP1* RNAi transformants T2, T3 and T4 on cellophane membranes at 48 h. Data are mean percentages based on > 100 spores per replicate, three replicates per genotype. Error bars = 1 SE. (c–f) Phase-contrast micrographs showing the morphology of germlings of the wild-type (c) or *ChELP1* RNAi transformant T3 (d–f) growing on cellophane membranes. Bars, 10 μm. (c) Normal germination producing one germ tube (arrowhead) and one appressorium (arrow). (d) Abnormal germination producing two germ tubes and two appressoria from one spore. (e) Abnormal germination producing a bifurcated germ tube and two appressoria. (f) Abnormal lateral emergence of a secondary germ tube (arrowhead) from the side of the appressorium (arrow). (g, h) Quantification of morphological abnormalities in germlings of the wild-type or *ChELP1* RNAi transformants T2, T3 and T4 on cellophane membranes at 48 h. Data are mean percentages based on counting > 100 spores per replicate, three replicates per genotype. Error bars = 1 SE. (g) Histogram showing the proportion of germinated spores producing one germ tube with one appressorium (black bars), a bifurcated germ tube with two appressoria (white bars), or two germ tubes and two appressoria (grey bars). (h) Histogram showing the proportion of appressoria undergoing lateral germination to form secondary germ tubes growing on the cellophane surface.

The infection biology of *C. higginsianum* differs significantly from that of the three other plant pathogens from which LysM effectors were characterized. *C. fulvum* and *M. graminicola* both invade through stomata and develop exclusively as intercellular mycelia, so that molecular communication between host and pathogen is confined to the apoplast, and they do not differentiate specialized cell types to colonize plant tissues (Duncan & Howard, 2000; Thomma *et al.*, 2005). Infection by *C. higginsianum* is more similar to rice infection by *M. oryzae*, as both fungi produce melanized appressoria that penetrate living epidermal cells directly and intracellular biotrophic hyphae that grow in intimate contact with the plant plasma membrane (O'Connell *et al.*, 2004; Giraldo & Valent, 2013). However, in contrast to *M. oryzae*, *C. higginsianum* undergoes a clear and complete switch to destructive necrotrophy, associated with a striking change in morphology from bulbous pseudohyphae to thin filamentous hyphae.

A distinguishing feature of *ChELP1* and *ChELP2* is their preferential expression during biotrophy, with ChELP2 protein concentrated on the surface of biotrophic primary hyphae but not detectable on necrotrophic secondary hyphae. Moreover, there is an abrupt transition in labelling of ChELP2 where necrotrophic hyphae emerge from the biotrophic hyphae. This suggests that down-regulation of *ChELP2* during this morphological transition is more sharply delineated than is apparent from transcript profiling, or that the secreted ChELP becomes sequestered into the walls of biotrophic hyphae, leaving little free protein available for binding necrotrophic hyphae. Interestingly, in colocalization experiments, the presence of ChELP2 precisely correlated with the absence of chitin labelling by WGA. We cannot exclude the possibility that during the biotrophic phase, a portion of the cell wall chitin becomes deacetylated into chitosan, as proposed for *C. graminicola* based on the immunolabelling of chitosan (El Gueddari *et al.*, 2002). However, acetylated chitin is clearly present in *C. higginsianum* biotrophic hyphae, because WGA labelled the walls of cross-sectioned hyphae. Our results suggest that in biotrophic hyphae, but not necrotrophic hyphae, chitin is inaccessible to externally applied WGA as a result of masking by other wall components, such as ChELP2. The selective deployment of ChELP proteins during biotrophy suggests that chitin protection or evasion of chitin-triggered immunity is critically important when the fungus grows in intimate contact with living host cells, but is no longer necessary during necrotrophic growth, when host cells are rapidly killed ahead of infection (O'Connell *et al.*, 2004).

We found that RNAi-mediated gene silencing of both *ChELP1* and *ChELP2* strongly impaired fungal virulence on susceptible *Arabidopsis* plants, with a 30-fold reduction in appressorial penetration frequency and a 50-fold reduction in fungal biomass. This severe virulence phenotype was not simply a result of reduced fungal fitness, as *in vitro* mycelial growth of the RNAi mutants was unaffected. Among plant pathogenic fungi, two distinct functions have so far been elucidated for fungal secreted LysM effectors, namely the protection of fungal chitin from attack by plant chitinases, as shown for *M. graminicola* Mg1LysM and Mg3LysM, and interference with chitin-induced host immune responses, as shown for *C. fulvum* Ecp6, *M. oryzae* Slp1 and *M. graminicola* Mg3LysM (de Jonge *et al.*, 2010; Marshall *et al.*, 2011; Mentlak *et al.*, 2012). These LysM effectors were proposed to sequester wall-derived chitin fragments to prevent chitin binding to host immune receptors. In addition, Ecp6 may prevent the dimerization of plant chitin receptors (Sánchez-Vallet *et al.*, 2013) required for the activation of immune signalling in *Arabidopsis* (Liu *et al.*, 2012).

Our findings that ChELP1 and ChELP2 bind fungal cell wall chitin *in vitro*, and that ChELP2 coats the cell walls of biotrophic hyphae, correlated with the reduced accessibility of chitin to WGA in these hyphae, are consistent with the possibility that ChELPs function to shield chitin from hydrolysis by plant chitinases during biotrophy. However, preincubation with recombinant ChELP1 and ChELP2 failed to protect *Trichoderma* germlings from the inhibitory effects of tomato chitinases, suggesting the *Colletotrichum* proteins do not have protective activity, in contrast to *Cladosporium* Avr4 (van den Burg *et al.*, 2006) and *Mycosphaerella* Mg1LysM and Mg3LysM (Marshall *et al.*, 2011). Nevertheless, it should be noted that chitin is located in the innermost layer of the fungal wall, close to the plasma membrane where it is synthesized (Bowman & Free, 2006). *In vivo*, ChELPs could bind chitin immediately upon their secretion to the extracellular space, which may protect chitin from chitinases more effectively than exogenous protein applied to the hyphal surface. Therefore, based on this *in vitro* assay alone, we cannot exclude the possibility that ChELPs play a role in chitinase protection during infection.

A second possibility is that ChELP1 and ChELP2 function to suppress chitin-triggered immunity by scavenging chitin fragments and thereby competing with plant chitin receptors, which is a conserved function of LysM effectors from three different fungal plant pathogens (de Jonge *et al.*, 2010; Marshall *et al.*, 2011; Mentlak *et al.*, 2012; Sánchez-Vallet *et al.*, 2013). We obtained evidence that ChELP1 and ChELP2 do play such a role, because in *Arabidopsis* seedlings they suppressed the rapid chitin-induced activation of the immune-related MAP kinases MPK3 and MPK6 (Miya *et al.*, 2007). Consistent with this, ChELP1 also inhibited the chitin-induced alkalinization of tomato cell cultures, but in this assay ChELP2 itself induced alkalinization. Given that *C. higginsianum* is not a pathogen of tomato, it is possible that ChELP2 is recognized by tomato cells, leading to activation of plant defense responses, whereas in the true host *Arabidopsis* both ChELP1 and ChELP2 may function to suppress chitin-induced immunity.

It was previously shown that the pathogenicity defect of *M. oryzae slp1*-targeted mutants could be complemented on rice plants in which the chitin receptor CEBiP1 was silenced by RNAi (Mentlak *et al.*, 2012). Similarly, pathogenicity of the *Mycosphaerella* Mg3LysM deletion mutant was fully restored on wheat plants in which expression of CEBiP or CERK1 orthologues was suppressed by virus-induced gene silencing (Lee *et al.*, 2014). In *Arabidopsis*, two plasma membrane-resident pattern recognition receptors are known to mediate independent chitin perception pathways, leading to resistance against fungal pathogens, namely LYK1/CERK1 and the CEBiP homologue

LYM2 (Miya *et al.*, 2007; Shinya *et al.*, 2012; Faulkner *et al.*, 2013; Cao *et al.*, 2014). However, the virulence of *ChELP1/2* mutants was not complemented on *Arabidopsis* plants lacking either one of these chitin receptors. Given the failure of the mutants to penetrate not only host epidermal cells but also inert cellophane membranes, the most likely explanation is that silencing *ChELP1/2* abolishes the penetration ability of appressoria in a plant-independent manner. Consistent with this hypothesis, we found that germlings of the *ChELP1/2* mutants displayed a range of morphological abnormalities, including the lateral emergence of secondary germ tubes from appressoria, which is also a phenotype of penetration-deficient melanin biosynthesis mutants in other *Colletotrichum* species (Kubo *et al.*, 1982). Interestingly, although *M. oryzae* elaborates structurally similar appressoria for host cell entry, deletion of the *Slp1* LysM effector did not impact appressorium morphogenesis or penetration ability on rice (Mentlak *et al.*, 2012). Taken together, our data suggest that specific induction of *ChELP1* and *ChELP2* at the biotrophic stage *in planta* may be critical for suppressing chitin-triggered immune responses, while the basal expression levels in appressoria *in vitro* and *in planta* are required for efficient substrate penetration. Further work is now needed to elucidate how these chitin-binding proteins contribute to appressorial function and the switch to invasive hyphal growth.

Author contributions

R.J.O. and H.T. initiated the project. R.J.O., S.H., H.T., B.P.H.J.T., N.S. and E.K. planned and designed the research. H.T., S.H., A.K., H.B.H., V.H., G.P.R., K.H., R.J.O., U.N. and T.S. performed experiments. S.H., H.T., A.K., V.H., G.P.R., K.H., R.J.O., E.K. and N.S. analysed the data. S.H., G.P.R., A.K., H.T., H.B.H., V.H. and U.N. prepared the figures and tables. R.J.O., S.H. and B.P.H.J.T. wrote the manuscript.

References

Al Atalah B, Fouquaert E, Vanderschaeghe D, Proost P, Balzarini J, Smith DF, Rougé P, Lasanajak Y, Callewaert N, Van Damme EJ. 2011. Expression analysis of the nucleocytoplasmic lectin 'Orysata' from rice in *Pichia pastoris*. *FEBS Journal* **278**: 2064–2079.

Blixt O, Head S, Mondala T, Scanlan C, Huflejt ME, Alvarez R, Bryan MC, Fazio F, Calarese D, Stevens J et al. 2004. Printed covalent glycan array for ligand profiling of diverse glycan binding proteins. *Proceedings of the National Academy of Sciences, USA* **101**: 17033–17038.

Bolton MD, van Esse HP, Vossen JH, de Jonge R, Stergiopoulos I, Stulemeijer IJ, van den Berg GC, Borrás-Hidalgo O, Dekker HL, de Koster CG et al. 2008. The novel *Cladosporium fulvum* lysin motif effector Ecp6 is a virulence factor with orthologues in other fungal species. *Molecular Microbiology* **69**: 119–136.

Bowman SM, Free SJ. 2006. The structure and synthesis of the fungal cell wall. *BioEssays* **28**: 799–808.

van den Burg HA, Harrison SJ, Joosten MH, Vervoort J, de Wit PJ. 2006. *Cladosporium fulvum* Avr4 protects fungal cell walls against hydrolysis by plant chitinases accumulating during infection. *Molecular Plant–Microbe Interactions* **19**: 1420–1430.

Cao Y, Liang Y, Tanaka K, Nguyen CT, Jedrzejczak RP, Joachimiak A, Stacey G. 2014. The kinase LYK5 is a major chitin receptor in *Arabidopsis* and forms a chitin-induced complex with related kinase CERK1. *eLife* **3**: e03766.

Chen XL, Shi T, Yang J, Shi W, Gao X, Chen D, Xu X, Xu JR, Talbot NJ, Peng YL. 2014. N-glycosylation of effector proteins by an α-1,3-mannosyltransferase is required for the rice blast fungus to evade host innate immunity. *Plant Cell* **26**: 1360–1376.

Dodds PN, Rathjen JP. 2010. Plant immunity: towards an integrated view of plant-pathogen interactions. *Nature Reviews Genetics* **11**: 539–548.

Duncan KE, Howard RJ. 2000. Cytological analysis of wheat infection by the leaf blotch pathogen *Mycosphaerella graminicola*. *Mycological Research* **104**: 1074–1082.

Duplessis S, Hacquard S, Delaruelle C, Tisserant E, Frey P, Martin F, Kohler A. 2011. *Melampsora larici-populina* transcript profiling during germination and timecourse infection of poplar leaves reveals dynamic expression patterns associated with virulence and biotrophy. *Molecular Plant–Microbe Interactions* **24**: 808–818.

El Gueddari NE, Rauchhaus U, Moerschbacher BM, Deising HB. 2002. Developmentally regulated conversion of surface-exposed chitin to chitosan in cell walls of plant pathogenic fungi. *New Phytologist* **156**: 103–112.

van Esse HP, Bolton MD, Stergiopoulos I, De Wit PJGM, Thomma BPHJ. 2007. The chitin-binding *Cladosporium fulvum* effector protein Avr4 is a virulence factor. *Molecular Plant–Microbe Interactions* **20**: 1092–1101.

Faulkner C, Petutschnig E, Benitez-Alfonso Y, Beck M, Robatzek S, Lipka V, Maule AJ. 2013. LYM2-dependent chitin perception limits molecular flux via plasmodesmata. *Proceedings of National Academy of Sciences, USA* **110**: 9166–9170.

Felix G, Regenass M, Boller T. 1993. Specific perception of subnanomolar concentrations of chitin fragments by tomato cells: induction of extracellular alkalinisation, changes in protein phosphorylation, and establishment of a refractory state. *Plant Journal* **4**: 307–316.

Gan P, Ikeda K, Irieda H, Narusaka M, O'Connell RJ, Narusaka Y, Takano Y, Kubo Y, Shirasu K. 2013. Comparative genomic and transcriptomic analyses reveal the hemibiotrophic stage shift of *Colletotrichum* fungi. *New Phytologist* **197**: 1236–1249.

Giraldo MC, Valent B. 2013. Filamentous plant pathogen effectors in action. *Nature Reviews Microbiology* **11**: 800–814.

Gow NAR, Gooday GW, Newman RJ, Gull K. 1980. Ultrastructure of the septum in *Candida albicans*. *Current Microbiology* **4**: 357–359.

Hacquard S, Joly DL, Lin YC, Tisserant E, Feau N, Delaruelle C, Legué V, Kohler A, Tanguay P, Petre B et al. 2012. A comprehensive analysis of genes encoding small secreted proteins identifies candidate effectors in *Melampsora larici-populina* (poplar leaf rust). *Molecular Plant–Microbe Interactions* **25**: 279–293.

Hacquard S, Kracher B, Hiruma K, Münch PC, Garrido-Oter R, Weimann A, Thon MR, Damm U, Dallery JF, Hainaut M et al. 2016. Survival trade-offs in plant roots during colonization by closely related beneficial and pathogenic fungi. *Nature Communications*. doi: 10.1038/ncomms11362.

Howard RJ, Ferrari MA, Roach DH, Money NP. 1991. Penetration of hard substrates by a fungus employing enormous turgor pressures. *Proceedings of the National Academy of Sciences, USA* **88**: 11281–11284.

Huser A, Takahara H, Schmalenbach W, O'Connell R. 2009. Discovery of pathogenicity genes in the crucifer anthracnose fungus *Colletotrichum higginsianum*, using random insertional mutagenesis. *Molecular Plant-Microbe Interactions* 22: 143–156.

de Jonge R, Thomma BPHJ. 2009. Fungal LysM effectors: extinguishers of host immunity? *Trends in Microbiology* 17: 151–157.

de Jonge R, van Esse HP, Kombrink A, Shinya T, Desaki Y, Bours R, van der Krol S, Shibuya N, Joosten MH, Thomma BP. 2010. Conserved fungal LysM effector Ecp6 prevents chitin-triggered immunity in plants. *Science* 329: 953–955.

Joosten MHAJ, Verbakel HM, Nettekoven ME, Van Leeuwen J, Van der Vossen RTM, De Wit PJGM. 1995. The phytopathogenic fungus *Cladosporium fulvum* is not sensitive to the chitinase and ß-1,3-glucanase defence proteins of its host, tomato. *Physiological and Molecular Plant Pathology* 46: 45–59.

Kaku H, Nishizawa Y, Ishii-Minami N, Akimoto-Tomiyama C, Dohmae N, Takio K, Minami E, Shibuya N. 2006. Plant cells recognize chitin fragments for defense signaling through a plasma membrane receptor. *Proceedings of the National Academy of Sciences, USA* 103: 11086–11091.

Kleemann J, Rincon-Rivera LJ, Takahara H, Neumann U, van Themaat EV, van der Does HC, Hacquard S, Stüber K, Will I, Schmalenbach W et al. 2012. Sequential delivery of host-induced virulence effectors by appressoria and intracellular hyphae of the phytopathogen *Colletotrichum higginsianum*. *PLoS Pathogens* 8: e1002643.

Koharudin LM, Viscomi AR, Montanini B, Kershaw MJ, Talbot NJ, Ottonello S, Gronenborn AM. 2011. Structure-function analysis of a CVNH-LysM lectin expressed during plant infection by the rice blast fungus *Magnaporthe oryzae*. *Structure* 19: 662–674.

Kubo Y, Suzuki K, Furusawa I, Ishida N, Yamamoto M. 1982. Relation of appressorium pigmentation and penetration of nitrocellulose membranes by *Colletotrichum lagenarium*. *Phytopathology* 72: 498–501.

Larkin MA, Blackshields G, Brown NP, Chenna R, McGettigan PA, McWilliam H, Valentin F, Wallace IM, Wilm A, Lopez R et al. 2007. Clustal W and Clustal X version 2.0. *Bioinformatics* 23: 2947–2948.

Lee WS, Rudd JJ, Hammond-Kosack KE, Kanyuka K. 2014. *Mycosphaerella graminicola* LysM effector-mediated stealth pathogenesis subverts recognition through both CERK1 and CEBiP homologues in wheat. *Molecular Plant-Microbe Interactions* 27: 236–243.

Liu T, Liu Z, Song C, Hu Y, Han Z, She J, Fan F, Wang J, Jin C, Chang J et al. 2012. Chitin-induced dimerization activates a plant immune receptor. *Science* 336: 1160–1164.

Lu X, Tintor N, Mentzel T, Kombrink E, Boller T, Robatzek S, Schulze-Lefert P, Saijo Y. 2009. Uncoupling of sustained MAMP receptor signaling from early outputs in an *Arabidopsis* endoplasmic reticulum glucosidase II allele. *Proceedings of the National Academy of Sciences, USA* 106: 22522–22527.

Marshall R, Kombrink A, Motteram J, Loza-Reyes E, Lucas J, Hammond-Kosack KE, Thomma BP, Rudd JJ. 2011. Analysis of two *in planta* expressed LysM effector homologs from the fungus *Mycosphaerella graminicola* reveals novel functional properties and varying contributions to virulence on wheat. *Plant Physiology* 156: 756–769.

Mentlak TA, Kombrink A, Shinya T, Ryder LS, Otomo I, Saitoh H, Terauchi R, Nishizawa Y, Shibuya N, Thomma BP et al. 2012. Effector-mediated suppression of chitin-triggered immunity by *Magnaporthe oryzae* is necessary for rice blast disease. *Plant Cell* 24: 322–335.

Micali CO, Neumann U, Grunewald D, Panstruga R, O'Connell R. 2011. Biogenesis of a specialized plant-fungal interface during host cell internalization of *Golovinomyces orontii* haustoria. *Cellular Microbiology* 13: 210–226.

Miya A, Albert P, Shinya T, Desaki Y, Ichimura K, Shirasu K, Narusaka Y, Kawakami N, Kaku H, Shibuya N. 2007. CERK1, a LysM receptor kinase, is essential for chitin elicitor signaling in *Arabidopsis*. *Proceedings of the National Academy of Sciences, USA* 104: 19613–19618.

Narusaka Y, Shinya T, Narusaka M, Motoyama N, Shimada H, Murakami K, Shibuya N. 2013. Presence of LYM2 dependent but CERK1 independent disease resistance in *Arabidopsis*. *Plant Signaling & Behavior* 8: e25345.

O'Connell R, Herbert C, Sreenivasaprasad S, Khatib M, Esquerré-Tugayé MT, Dumas B. 2004. A novel *Arabidopsis-Colletotrichum* pathosystem for the molecular dissection of plant–fungal interactions. *Molecular Plant-Microbe Interactions* 17: 272–282.

O'Connell RJ, Ride JP. 1990. Chemical detection and ultrastructural localization of chitin in cell walls of *Colletotrichum lindemuthianum*. *Physiological and Molecular Plant Pathology* 37: 39–53.

O'Connell RJ, Thon MR, Hacquard S, Amyotte SG, Kleemann J, Torres MF, Damm U, Buiate EA, Epstein L, Alkan N et al. 2012. Lifestyle transitions in plant pathogenic *Colletotrichum* fungi deciphered by genome and transcriptome analyses. *Nature Genetics* 44: 1060–1065.

Pain NA, O'Connell RJ, Mendgen K, Green JR. 1994. Identification of glycoproteins specific to biotrophic intracellular hyphae formed in the *Colletotrichum lindemuthianum*-bean interaction. *New Phytologist* 127: 233–242.

Perfect SE, O'Connell RJ, Green EF, Doering-Saad C, Green JR. 1998. Expression cloning of a fungal proline-rich glycoprotein specific to the biotrophic interface formed in the *Colletotrichum*-bean interaction. *Plant Journal* 15: 273–279.

Perfect SE, Pixton KL, O'Connell RJ, Green JR. 2000. The distribution and expression of a biotrophy-related gene, *CIH*, within the genus *Colletotrichum*. *Molecular Plant Pathology* 1: 213–221.

Petersen TN, Brunak S, von Heijne G, Nielsen H. 2011. SignalP 4.0: discriminating signal peptides from transmembrane regions. *Nature Methods* 8: 785–786.

Punta M, Coggill PC, Eberhardt RY, Mistry J, Tate J, Boursnell C, Pang N, Forslund K, Ceric G, Clements J et al. 2012. The Pfam protein families database. *Nucleic Acids Research* 40: D290–D301.

Rafiqi M, Jelonek L, Akum NF, Zhang F, Kogel KH. 2013. Effector candidates in the secretome of *Piriformospora indica*, a ubiquitous plant-associated fungus. *Frontiers in Plant Science* 4: 228.

Sánchez-Vallet A, Mesters JR, Thomma BP. 2015. The battle for chitin recognition in plant-microbe interactions. *FEMS Microbiology Reviews* 39: 171–83.

Sánchez-Vallet A, Saleem-Batcha R, Kombrink A, Hansen G, Valkenburg DJ, Thomma BP, Mesters JR. 2013. Fungal effector Ecp6 outcompetes host immune receptor for chitin binding through intrachain LysM dimerization. *elife* 2: e00790.

Sawaguchi A, Ide S, Goto Y, Kawano J, Oinuma T, Suganuma T. 2001. A simple contrast enhancement by potassium permanganate oxidation for Lowicryl K4M ultrathin sections prepared by high pressure freezing/freeze substitution. *Journal of Microscopy* 201: 77–83.

Shinya T, Motoyama N, Ikeda A, Wada M, Kamiya K, Hayafune M, Kaku H, Shibuya N. 2012. Functional characterization of CEBiP and CERK1 homologs in *Arabidopsis* and rice reveals the presence of different chitin receptor systems in plants. *Plant and Cell Physiology* 53: 1696–1706.

Stergiopoulos I, de Wit PJ. 2009. Fungal effector proteins. *Annual Review of Phytopathology* 47: 233–263.

Sturn A, Quackenbush J, Trajanoski Z. 2002. Genesis: cluster analysis of microarray data. *Bioinformatics* 18: 207–208.

Takahara H, Dolf A, Endl E, O'Connell R. 2009. Flow cytometric purification of *Colletotrichum higginsianum* biotrophic hyphae from *Arabidopsis* leaves for stage-specific transcriptome analysis. *Plant Journal* 59: 672–683.

Tamura K, Dudley J, Nei M, Kumar S. 2007. MEGA4: Molecular Evolutionary Genetics Analysis (MEGA) software version 4.0. *Molecular Biology and Evolution* 24: 1596–1599.

Thomma BPHJ, van Esse HP, Crous PW, De Wit PJGM. 2005. *Cladosporium fulvum* (syn. *Passalora fulva*), a highly specialized plant pathogen as a model for functional studies on plant pathogenic Mycosphaerellaceae. *Molecular Plant Pathology* 6: 379–393.

Tsuda K, Sato M, Stoddard T, Glazebrook J, Katagiri F. 2009. Network properties of robust immunity in plants. *PLoS Genetics* 5: e1000772.

Waterhouse AM, Procter JB, Martin DMA, Clamp M, Barton GJ. 2009. Jalview Version 2 – a multiple sequence alignment editor and analysis workbench. *Bioinformatics* 25: 1189–1191.

Zuccaro A, Lahrmann U, Güldener U, Langen G, Pfiffi S, Biedenkopf D, Wong P, Samans B, Grimm C, Basiewicz M et al. 2011. Endophytic life strategies decoded by genome and transcriptome analyses of the mutualistic root symbiont *Piriformospora indica*. *PLoS Pathogens* 7: e1002290.

Supporting Information

Additional Supporting Information may be found online in the supporting information tab for this article:

Fig. S1 Sequence similarities among ChELP1, ChELP2 and other characterized fungal extracellular LysM proteins.

Fig. S2 Analysis of ChELP proteins expressed in *Pichia pastoris* and *Escherichia coli* for cross-reactivity with monoclonal antibody UB25 and predicted glycosylation.

Fig. S3 ChELP1 and ChELP2 cannot protect fungal hyphae from hydrolysis by tomato chitinases.

Fig. S4 ChELP1, but not ChELP2, suppresses chitin-triggered plant immune responses.

Fig. S5 Silencing of *ChELP1*.

Fig. S6 Expression levels of *ChELP1*, *ChELP2* and the control genes *ChG6PDH* (glucose-6-phosphate dehydrogenase), *ChElF* (translation elongation factor) and *ChEMP1* (Extracellular Matrix Protein 1).

Fig. S7 Appressorium turgor pressure is not affected by silencing *ChELP1/2*.

Fig. S8 Appressorium ultrastructure is not affected by silencing *ChELP1/2*.

Table S1 Primers used for qPCR and RT-qPCR

Table S2 Summary of *Colletotrichum higginsianum* LysM domain-containing proteins

Table S3 Glycan identities

Methods S1 Expression of recombinant ChELP1 and ChELP2 proteins.

Methods S2 SDS-PAGE and western blotting.

Methods S3 Detection of mannosylation by sidechain modification.

Please note: Wiley Blackwell are not responsible for the content or functionality of any supporting information supplied by the authors. Any queries (other than missing material) should be directed to the *New Phytologist* Central Office.